

Stress distribution in particulate filled composites and its effect on micromechanical deformation

G. VÖRÖS

Eötvös University Budapest, Institute for General Physics, H-1445 Budapest, P.O. Box 323, Hungary

B. PUKÁNSZKY

Central Research Institute for Chemistry, Hungarian Academy of Sciences, 1525 Budapest, P.O. Box 17, Hungary

A model was developed which assumes the spontaneous formation of an interphase around the inclusions in particulate filled composites. Elastic properties of the interphase change continuously from the surface of the particle to a matrix value far from it. Using first-order perturbation calculations an approximate analytical solution was given for the distribution of displacements and stresses around the inclusions. Fitting the model to experimental data has shown that an appropriate choice for the function and the parameters describing property changes around the inclusions makes possible the reliable prediction of composite properties. Using a simple averaging procedure, composition dependence of tensile yield stress was described; in accordance with experimental observations the model could predict composite yield stresses exceeding the matrix value and explain the effect of interfacial interactions. Comparison of the theoretical model with a previously developed semi-empirical one indicates that the main factor determining yield stress is the relative load bearing capacity of the second component. Interacting stress fields compensate each other, decreasing local stress maxima; thus justifying the averaging procedure applied. Contradictions of the models are analysed and areas for further research are also indicated in the paper.

1. Introduction

In heterogeneous polymer systems stress distribution around the particles determines micromechanical deformations and as a consequence macroscopic properties and performance of the material [1, 2]. The basic micromechanical deformations of polymers, shear yielding and crazing, may be accompanied by debonding in particulate filled composites [3–5]. Earlier studies have shown that the initiation of shear yielding and crazing depends on the local stress distribution, which is modified by thermal stresses [6]. Debonding, however, is influenced also by matrix–filler, *m–f*, interaction, which is determined by the strength of the interaction and the size of the inclusions [4, 6, 7]. Thus, the three main factors determining stress distribution and the prevailing deformation mechanism are stress concentration, thermal stresses and interaction [4–8].

In order to determine the distribution of stresses and local stress maxima around the particles, stress analysis has to be carried out. Application of traditional stress analysis (e.g. Goodier [9]) for the determination of stress distribution and for calculation of the initiation criteria of the different micromechanical processes (shear yielding, crazing, debonding) leaves

some phenomena occurring in heterogeneous polymer systems unexplained [6], i.e.

1. composite yield stresses exceeding that of the matrix (Fig. 1) [6, 10, 11],
2. particle size dependence of properties (Fig. 1) [10–13],
3. effect of interacting stress fields of neighbouring particles, and
4. interfacial interactions [12].

Since in particulate filled thermoplastics interaction of the components leads to the development of an interphase which has properties different from those of both components [14, 15], a model has to be used in the stress analysis which takes this phenomenon into account.

Several attempts have been already made to predict the elastic properties of composites by introducing an interphase layer of definite thickness and properties, which is independent from the position inside the layer [16–18]. These models assume uniform deformation both in the matrix and in the interlayer. In the case of a spontaneously formed interphase, a continuous change of elastic properties must occur in the interlayer from a higher value at the surface to matrix characteristics at a certain distance from the particle.

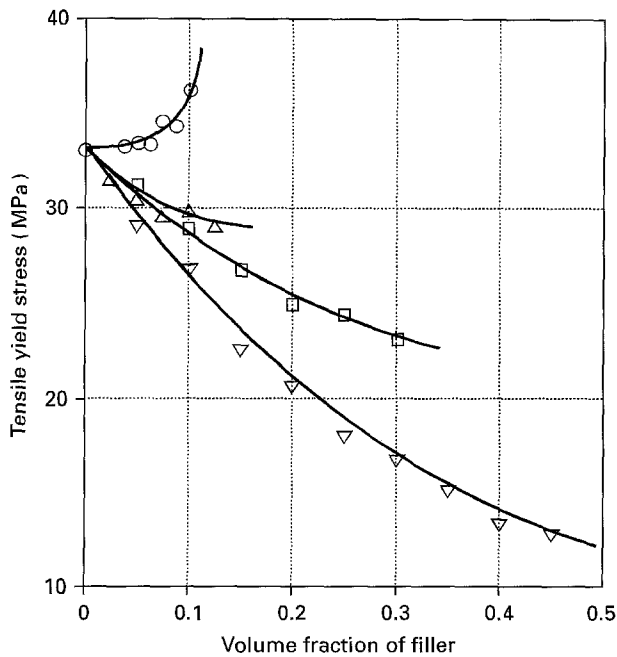


Figure 1 Tensile yield stress of particulate filled PP composites plotted against filler content. Effect of filler particle size: (∇) 58.0 μm , (\square) 3.6 μm , (\triangle) 0.08 μm , (\circ) 0.01 μm .

In the authors' calculations the existence of such an interlayer is assumed and with the help of first-order perturbation calculations an approximate analytical solution is given for the determination of stresses inside and outside the particles. The results of the analysis are used in a simple averaging procedure and by choosing the proper dependence of elastic properties on the distance from the particle, compositional dependence of tensile yield stress is predicted. Results of the calculations are compared with experimental data; attention is called to the contradictions of the model and areas for further research are indicated.

2. Experimental procedure

2.1. The model

A particle with radius, R , is placed into the origin of the co-ordinate system (Fig. 2). In the z -direction an external stress, σ^e , is applied which is homogeneous far from the particle. If the development of a spontaneously formed interphase with continuously changing properties is assumed, the equilibrium equation can be expressed as

$$\text{div } \hat{\sigma}(\mathbf{r}) = \text{div}[\hat{C}^0(\mathbf{r})\hat{\varepsilon}(\mathbf{r})] = 0 \quad (1)$$

and the constitutive equation is written in the form

$$\hat{C}(\mathbf{r}) = \hat{C}^0[1 + \eta(|\mathbf{r}|)] \quad (2)$$

where \hat{C}^0 is the homogeneous isotropic elastic property tensor of the matrix. The η function describes the change of elastic properties relative to the homogeneous \hat{C}^0 value far from the particle. $\eta = 0$ corresponds to the traditional two-phase models. Rearrangement of Equations 1 and 2 leads to

$$\text{div}(\hat{C}^0\hat{\varepsilon}) = -(\hat{C}^0\hat{\varepsilon}) \frac{\text{grad } \eta(|\mathbf{r}|)}{1 + \eta(|\mathbf{r}|)} \quad (3)$$

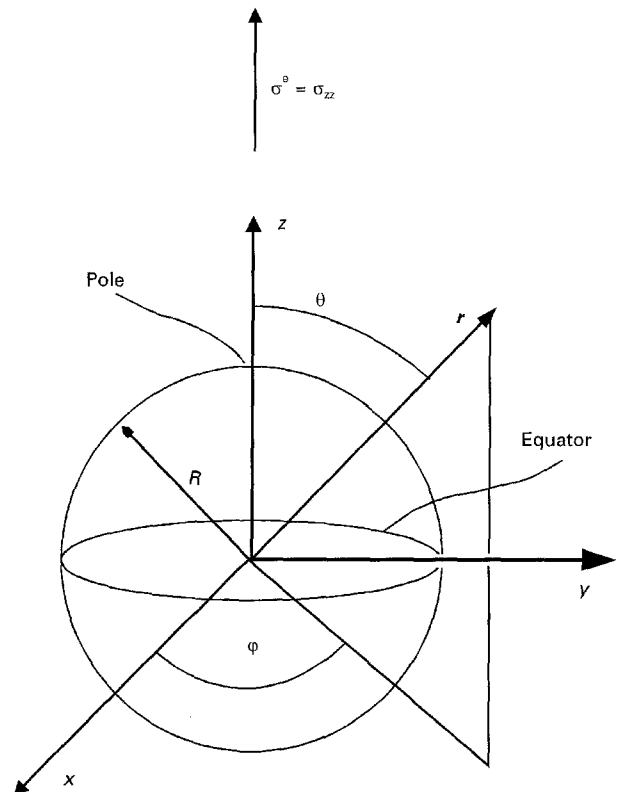


Figure 2 Spherical co-ordinate system used in the calculations.

The physical meaning of Equation 3 can be explained also by assuming that the effect of the interphase with changing properties induces a volume force field in a matrix with a homogeneous elastic modulus.

Perturbation in the elastic properties of the matrix caused by the presence of an inclusion decreases continuously with distance from the particle surface [16, 17, 19, 20]. The η function giving the spatial distribution of the elastic properties, as well as its gradient, appears on the right-hand side of Equation 3. In the model, η is not defined directly, but it is assumed that the right-hand side of Equation 3 can be given as the gradient of a ψ function. The grad ψ function must have the proper physical meaning and it should be expressed in a simple form. It can be proven that a proper selection of η yields a convergent solution; the most convenient form of the function was found to be

$$\frac{\text{grad } \eta(|\mathbf{r}|)}{1 + \eta(|\mathbf{r}|)} = \text{grad } \Psi(\mathbf{r}) = -\frac{K}{r} \left(\frac{R}{r}\right)^p \quad (4)$$

where K and p are dimensionless quantities which can be related to η by the integration of Equation 4, i.e.

$$\eta(|\mathbf{r}|) = \exp\left[\ln(J + 1) \left(\frac{R}{r}\right)^{p-1}\right] - 1 \quad (5)$$

and

$$K = (p - 1)\ln(J - 1) \quad (6)$$

K is a simple proportionality constant, while p determines the decrease of the grad ψ function (modulus) with increasing distance from the particle. K and p are constants, their values can be determined from experimental data. In Equation 6, J is an integration

constant having direct physical meaning, it defines the difference between the moduli on the surface of the particle and far from it in the matrix i.e.

$$J = \frac{E(R)}{E^0} - 1 = \frac{G(R)}{G^0} - 1 \quad (7)$$

Some characteristic $\eta(\rho, p, J)$ functions are presented in Fig. 3 ($\rho = r/R$). To create the curves of Fig. 3, p values were chosen which yield interphase thicknesses comparable with experience. Attention must be called here that Equation 7 indicates equal dependence of the two moduli on the distance from the particle and as a consequence Poisson's ratio, ν , is independent from location.

Expression for the displacement field is obtained by the combination of Equations 2-4 and 7

$$\begin{aligned} \text{grad div } \mathbf{u} + (1 - 2\nu)\Delta\mathbf{u} = & -2\nu \text{grad } \Psi(\mathbf{r}) \text{div } \mathbf{u}(\mathbf{r}) \\ & - 2(1 - 2\nu)\text{grad } \Psi(\mathbf{r}) \\ & \times \text{grad } \mathbf{u}(\mathbf{r}) \end{aligned} \quad (8)$$

The equation can be solved by iteration using the following function for the displacement vector

$$\mathbf{u}(\mathbf{r}) = \mathbf{u}^0(\mathbf{r}) + \mathbf{u}^1(\mathbf{r}) + \mathbf{u}^2(\mathbf{r}) + \dots + \mathbf{u}^n(\mathbf{r}) \dots \quad (9)$$

where $\mathbf{u}^0(\mathbf{r})$ is the solution of the $\text{grad div } \mathbf{u}(\mathbf{r}) + (1 - 2\nu)\Delta\mathbf{u} = 0$ equation describing the two-phase composite not containing an interphase (e.g. Goodier [9]). The $\mathbf{u}^1, \mathbf{u}^2, \mathbf{u}^3, \dots$, components are the corrections obtained in each iteration step. With the help of the Φ^n and \mathbf{A}^n vector potentials \mathbf{u}^n can be divided into two parts, i.e.

$$\mathbf{u}^n = \text{grad } \Phi^n(\mathbf{r}) + \text{curl } \mathbf{A}^n \quad (10)$$

Separating the displacement vector into the Φ^n and \mathbf{A}^n terms and starting with \mathbf{u}^0 , the Φ^n and \mathbf{A}^n components obtained in the n th iteration step can be expressed as

$$\Delta\Delta\Phi^n = \frac{1}{2(1 - \nu)} \text{div } \mathbf{f}^{n-1}(\mathbf{u}^{n-1}) \quad (11)$$

and

$$\Delta\Delta\mathbf{A}^n = \frac{1}{1 - 2\nu} \text{curl } \mathbf{f}^{n-1}(\mathbf{u}^{n-1}) \quad (12)$$

The equations were solved under the boundary conditions of

$$\mathbf{u}^{m,r}(R) = 0 \quad (13)$$

for a completely rigid particle and

$$(\hat{\sigma}^e + \hat{\sigma}^m)\mathbf{n} = \hat{\sigma}^f \mathbf{n} \quad (14)$$

expressing continuity of stresses. The equations can be expressed in analytical form by using spherical harmonic functions. Model calculations were carried out with one iteration step to determine $\mathbf{u} \approx \mathbf{u}^0 + \mathbf{u}^1$ in a polar co-ordinate system (see Fig. 2), where the z -axis was parallel with the direction of the external stress. The $(G^0/\sigma^e R) (\partial u_r/\partial \rho)$ component of the displacement field is plotted in Fig. 4 at $\theta = 0$ for different p values in the case of rigid particles ($J = 0.8$). $J = 0$ would correspond to a two-phase model with-

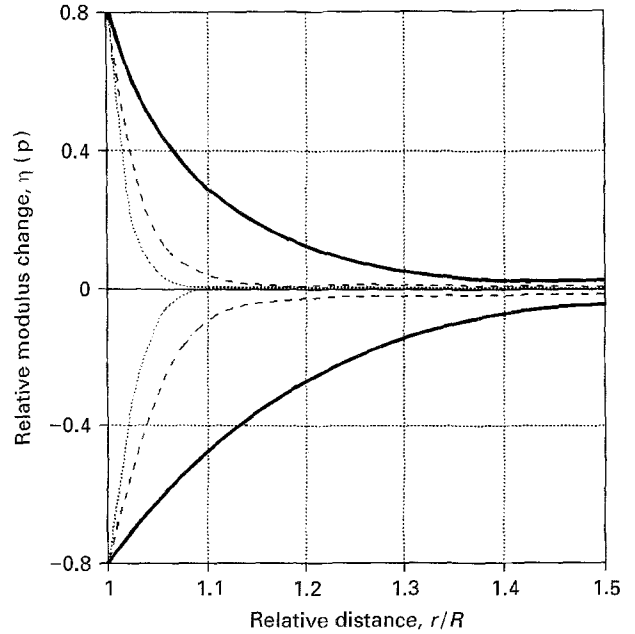


Figure 3 Changing elastic properties of the interphase as a function of the distance from the particle surface at different p (rate of property change) [(—) 10, (---) 30, (·····) 60] and $J = \pm 0.8$ (interphase property at the surface, $\theta = 0$) values.

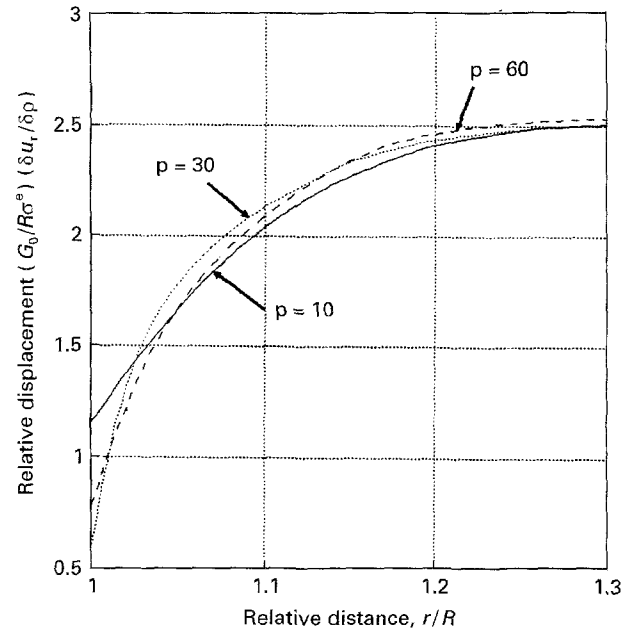


Figure 4 Effect of an interlayer with changing properties on the displacements around the particle under external load. Relative displacement is plotted against relative distance at different p values and at $J = 0.8, \theta = 0$.

out an interphase. Significant changes can be observed in displacement due to the presence of a hard interphase.

Stress fields can be derived from the deformations determined previously. Stress distribution around a particle is presented in Fig. 5, it depends very much on p , i.e. on the "thickness" of the interphase. Depending on p , the stress concentration can reach a value of about three compared to a stress concentration factor of about two obtained in the two-phase approach [9]. In the case of a thin interlayer, $p = 60$, stresses at the surface of the particle are lower than in the two-phase

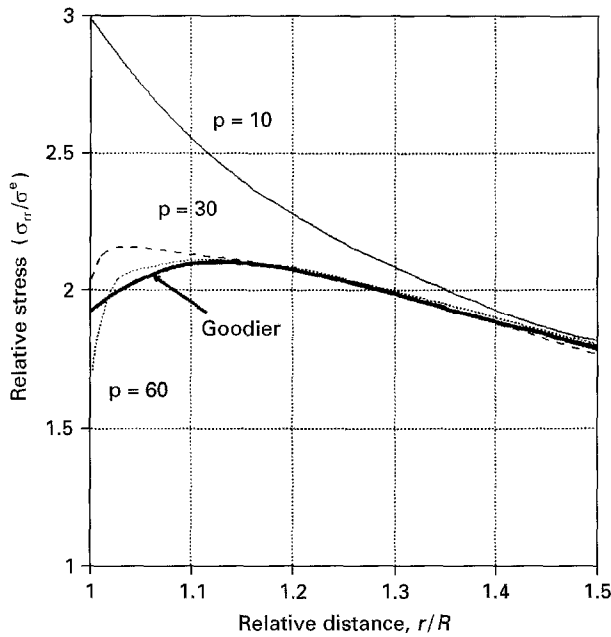


Figure 5 Radial stress distribution as a function of distance from the particle surface at different p values. $J = 0.8$, $\theta = 0$. Goodier's solution [9] represents a boundary case without interlayer.

solution due to decreased deformation, but their value rapidly increases to the level obtained without an interphase. At a long distance from the particle σ_{rr}/σ^e becomes one, i.e. stresses assume the value of the homogeneous matrix. In boundary cases ($p = 1$ or $J = 0$) the model yields the same solution as the traditional Goodier approach, which verifies the validity of the treatment.

2.2. Calculation of the yield stress: averaging

Compositional dependence of yield stress can be determined by a simple averaging technique. One assumes that filler content, ϕ_f , is not too high and the interaction of the interphases of different particles can be neglected. In this case the stress inside one particle, $\hat{\sigma}^i$, is equal to that of a particle placed into an infinite matrix, $\hat{\sigma}^\infty$

$$\hat{\sigma}^i \simeq \hat{\sigma}^\infty \quad (15)$$

where $\hat{\sigma}^\infty$ includes the external stress, $\hat{\sigma}^e$. Average stresses developing in the particles and in the matrix, respectively, must satisfy the conditions

$$\phi_f \langle \hat{\sigma}^i \rangle_f + (1 - \phi_f) \langle \hat{\sigma}^m \rangle_m = \hat{\sigma}^e$$

$$\langle \hat{\sigma}^m \rangle_m \neq \hat{\sigma}^e \quad (16)$$

where $\langle \hat{\sigma}^i \rangle_f$ and $\langle \hat{\sigma}^m \rangle_m$ are the average stresses inside the particle and in the matrix, respectively. According to Equation 16 the resulting average stress is $\hat{\sigma}^e$. Introduction of Equation 15 into Equation 16 and rearrangement leads to the following solution for the stress developing in the matrix

$$\langle \hat{\sigma}^m \rangle_m = \frac{\hat{\sigma}^e - \phi_f \langle \hat{\sigma}^\infty \rangle_f}{1 - \phi_f} \quad (17)$$

If the yield stress of the matrix polymer is σ_{y0} , shear yielding is initiated in the composite at $\langle \hat{\sigma}^m \rangle_m \approx \sigma_{y0}$.

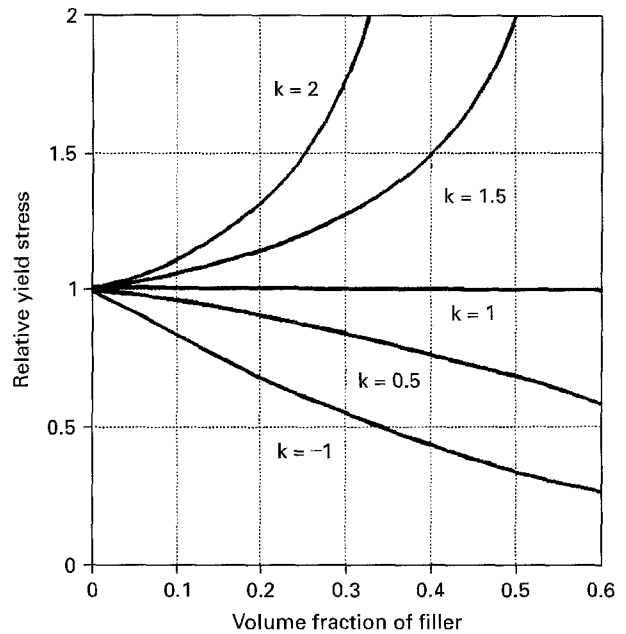


Figure 6 Compositional dependence of relative tensile yield stress of particulate filled composites predicted by Equation 18 at different degree of stress transfer, k .

The external stress initiating yielding can be expressed as

$$\sigma_y = \sigma_{y0} [1 - \phi_f / (1 - \phi_f \langle \sigma^\infty \rangle_f / \sigma^e)] \quad (18)$$

where $\langle \sigma^\infty \rangle_f / \sigma^e = k$ is a dimensionless quantity.

Equation 18 indicates that composite yield stress is determined by the average stress developing inside the particle. If, compared to the two-phase model, stresses change in the matrix, they will change also inside the particle due to the following boundary condition

$$[\hat{\sigma}^i(\rho = 1) + \hat{\sigma}^m(\rho = 1)] \mathbf{n} = 0 \quad (19)$$

This results in a change of composite yield stress as well.

Relative yield stress calculated according to Equation 18 is presented in Fig. 6. The figure closely resembles Fig. 1, where experimentally determined yield stress values are plotted as a function of composition for polypropylene(PP)/CaCO₃ composites. In the $\langle \sigma^\infty \rangle_f / \sigma^e = k = 1$ case, $\sigma_y = \sigma_{y0}$. If $k > 1$, yield stress increases continuously; while at $k < 1$ it decreases. The model obviously answers at least two of the questions presented in the introduction, it takes into account interfacial interactions and predicts composite yield stresses exceeding that of the matrix. Boundary cases yielding solutions equivalent to the traditional Goodier [9] solution and strong similarity of the compositional dependence of measured and calculated yield stresses supply sufficient proof for the validity of the approach.

3. Discussion

3.1. Verification: comparison of experimental data

The extremely simple form of Equation 18 makes comparison with experimental data easy. Rearrangement of the equation into

$$\frac{1 - \phi_f}{\sigma_y} = \frac{1}{\sigma_{y0}} - \frac{k}{\sigma_{y0}} \phi_f \quad (20)$$

and plotting $(1 - \phi_f)/\sigma_y$ versus ϕ_f should yield straight lines with an interception of $1/\sigma_{y0}$ and a slope of k/σ_{y0} . Indeed, plotting experimentally measured yield stresses of some PP/CaCO₃ composites [10–12] in the above-mentioned way excellent straight lines are obtained in practically all cases (Fig. 7). The three CaCO₃ fillers differ in particle size, i.e. specific surface area, while the matrix polymer is the same in all cases. Slopes of the lines differ significantly from each other indicating strong particle size dependence of parameter k , which is not predicted by the model. The fact, however, that the theoretically derived correlation predicts compositional dependence correctly and can be fitted to the experimental data is encouraging and further verifies the validity of the treatment.

Existing data on different particulate filled thermoplastic composites [10–12] have been analysed and the characteristic parameters calculated. The results are compiled in Table I. Dependence of k on specific surface area of the filler is clearly seen in Fig. 8. The correlation can be divided into two parts. In the first section k depends linearly on A_f , as was observed earlier for the B versus A_f correlation [11]. The slope seems to depend also on the properties of the matrix polymer. At high specific surface areas a strong deviation from linearity is observed due to aggregation of very small filler particles ($< 0.1 \mu\text{m}$). The observation is further supported by the k values obtained for the SiO₂ ($A_f = 200 \text{ m}^2 \text{ g}^{-1}$) filled composites not plotted in Fig. 8 (see Table I). The effect of filler characteristics depends strongly on matrix properties as well, which is in agreement with the physical meaning of k and emphasizes the importance of the relative load bearing capacity of the components. This latter factor depends on the properties of the components and on interfacial adhesion.

Since k is related both to the rate of property decrease, (“thickness” of the interphase, p) and to the

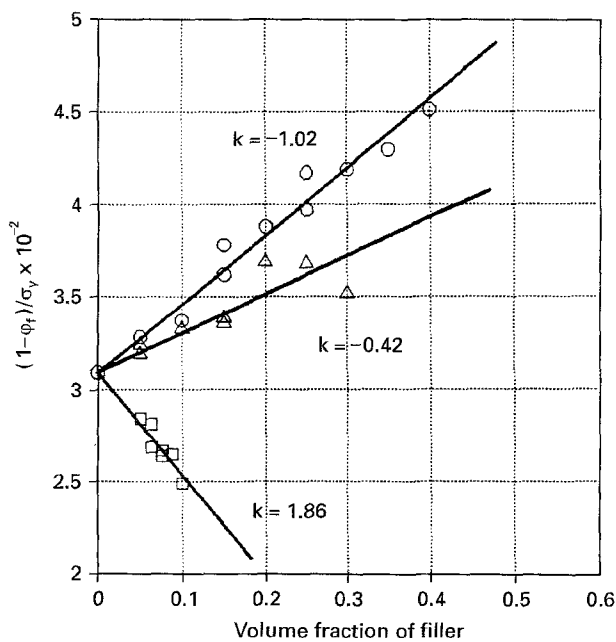


Figure 7 Tensile yield stress of PP composites plotted in a linearized form of Equation 18. Particle size: (○) 58.0 μm ; (Δ) 3.6 μm ; (\square) 0.08 μm .

TABLE I Parameters of the model

Matrix	Filler	A_f ($\text{m}^2 \text{ g}^{-1}$)	k	J
PP	CaCO ₃	0.5	-1.02	-0.40
	CaCO ₃	1.9	-0.72	0.05
	CaCO ₃	2.2	-0.63	0.11
	CaCO ₃	3.3	-0.42	0.25
	CaCO ₃	5.0	-0.01	0.47
	CaCO ₃	16.5	0.36	0.64
	SiO ₂	200.0	1.86	1.22
PVC	CaCO ₃	0.5	-1.69	-0.20
	CaCO ₃	3.3	-0.90	0.44
	CaCO ₃	16.5	-0.38	0.44
	SiO ₂	200.0	1.87	1.70
LDPE	CaCO ₃	0.5	0.05	0.13
	CaCO ₃	3.3	1.62	0.35
	CaCO ₃	16.5	2.22	0.41
	SiO ₂	200.0	3.85	0.60

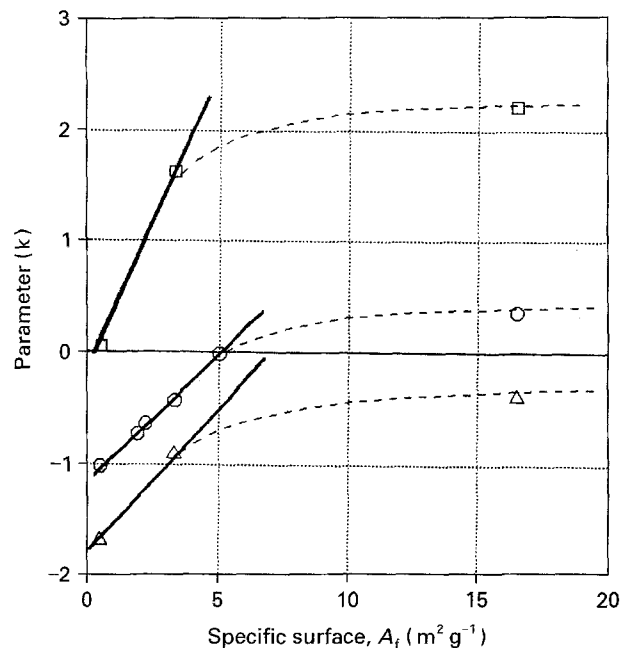


Figure 8 Dependence of k on the specific surface area of the filler. Effect of aggregation. Matrix polymer (Δ) PVC, (○) PP, (\square) LDPE.

property of the interphase (modulus on the surface of the particle, J) this latter parameter was also calculated and presented in Table I. In calculating J a constant relative interlayer thickness was assumed, i.e. $\rho = r/R \cong 1.1$. This could be achieved by choosing a p value of 60. A constant relative interlayer thickness means varying absolute thicknesses; on small particles a thinner, while on large particles a thicker, interphase forms.

The J values calculated in this way indicate strong variation of the interphase modulus on the specific surface area of the filler. In the case of large particles negative J values were calculated indicating a soft interlayer. Considering that in the investigated composites the interlayer forms spontaneously due to interaction created by secondary, van der Waals' forces, the strong particle size dependence and the formation of a soft interphase are difficult to explain. Adsorption

of polymers to fillers has been proved both directly and indirectly [21–23]. Theoretical calculations have also shown that adsorption of polymer molecules on a solid surface leads to ordered structures and decreased mobility, which indicates increased modulus at the same time [24]. Thus, the formation of a hard interphase seems to be more probable and instead of a constant relative interlayer thickness, a constant absolute interphase layer must be assumed in the calculations. Moreover, the values of Table I were calculated under the assumption that the dominating deformation mechanism is shear yielding, but obviously other mechanisms, especially debonding must be considered, as well.

In relation to the data of Table I, attention must be called to the fact that several factors were neglected during the development of the model and the calculations. The most important of these are

1. The effect of the interacting stress field of adjacent particles. The model assumes that interlayers of continuously changing properties formed around individual particles are independent from each other, but allows for interacting stress fields; it does not take them into account, however.

2. Local stress maxima are smoothed out by the averaging procedure. Although interaction of stress fields has such an effect, fluctuation of the stress field and local stress maxima still exist in the composite. These might induce local micromechanical deformations.

3. Several models predicting the compositional dependence of tensile yield stress use a minimum effective load bearing cross-section of the matrix, based on the argument that in the absence of interactions all the load is carried by the polymer [25–27]. The present model takes into account the average cross-section, which is proportional to the volume fraction of the matrix ($1 - \varphi_f$). Increased load at the minimum cross-section might induce yielding at lower external load than predicted by the model.

3.2. Comparison with an existing semiempirical model

By assuming the spontaneous formation of an interphase a somewhat different model was developed earlier for the prediction of the compositional dependence of the tensile yield stress of particulate filled polymer composites [10]. The only assumption of the model was that property (yield stress) changes proportionally to the amount of filler added. The final correlation is

$$\sigma_y = \sigma_{y0} \frac{1 - \varphi_f}{1 + 2.5\varphi_f} \exp(B\varphi_f) \quad (21)$$

where B is a parameter related to matrix–filler interaction. The correlation can be divided essentially into three parts: effect of matrix property, σ_{y0} ; effective load bearing cross-section, $(1 - \varphi_f) / (1 + 2.5\varphi_f)$; and interaction, $\exp(B\varphi_f)$. Comparison of the models and their parameters might help to explain the contradictions encountered during the application of the theor-

etical model to the experimental data, on the one hand, and to improve the understanding of the physical meaning of B , on the other.

General solutions of Equation 21 for different B values are plotted in Fig. 9. A very close similarity can be observed both with the predictions of the theoretical model (Fig. 7), and with the experimental data (Fig. 1). The semi-empirical model proved to be valid practically in all cases, not only in particulate filled composites, but also in other heterogeneous systems like polymer blends [28,29] as well. The similarity of Figs 7 and 9 predicts also some correlation between the parameters of the equations, i.e. k and B . Indeed, a perfect linear correlation exists between the two quantities shown by Fig. 10. Irrespectively of the matrix [PP, low density polyethylene (LDPE), polyvinylchloride (PVC)] or the characteristics of the filler (CaCO_3 , SiO_2 , changing particle size) the data fit the same line, suggesting that the models are complementary.

Beside the close correlation of the two models, Fig. 10 may lead us to further considerations. It is clear from the figure that B is always positive. This is in accordance with the assumption of the model; interaction leads always to stress-transfer and distribution of the load between the matrix and the filler. The load carried by the second component depends on the strength of the interaction and on the contact area (size of the interface), a correlation which could be expressed quantitatively by assuming that at a certain filler content all the polymer is bonded in the interphase (“maximum packing fraction”), i.e.

$$B = (1 + A_f l \rho_f) \ln \frac{\sigma_{yi}}{\sigma_{y0}} \quad (22)$$

where A_f is the specific surface area of the filler (size of the interface), ρ_f its density, while l and σ_{yi} are thickness and properties of the interphase, which depend

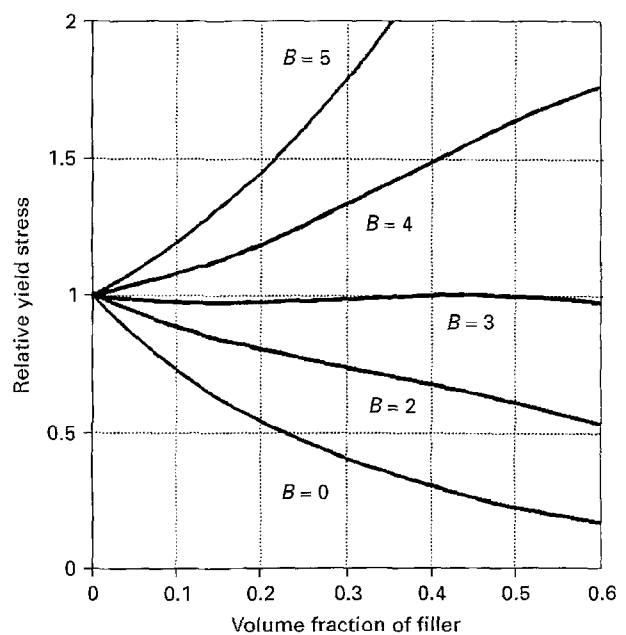


Figure 9 Compositional dependence of tensile yield stress of particulate filled composites predicted by Equation 21 for different matrix–filler interactions, B .

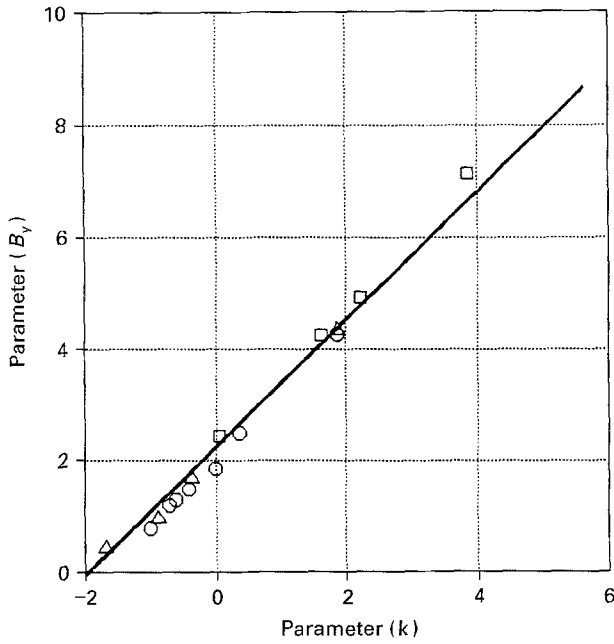


Figure 10 Correlation of parameters obtained from the theoretical Equation 18, k , and the semi-empirical model Equation 21 B , respectively. Particle size: (○) 58.0 μm , (△) 3.6 μm , (□) 0.08 μm .

on the strength of the interaction. Equation 22 was successfully used to explain the dependence of B , and thus σ_y , on particle size (A_f), interaction and matrix properties. The success of Equations 21 and 22 in the explanation of experimental data strengthens previous supposition that a hard interphase forms in the investigated particulate filled polymers. As a consequence, J must be calculated by assuming constant absolute layer thickness instead of the currently used relative one.

Although it was clear also earlier that B is proportional to stress transfer, i.e. to the load carried by the second component, the correlation of Fig. 10 further verifies this observation. Since B and k are in linear correlation and

$$k = f(J, p, E_f, E_m, G_f, G_m, \nu_f, \nu_m) \quad (23)$$

it is also valid that

$$B = f(J, p, E_f, E_m, G_f, G_m, \nu_f, \nu_m) \quad (24)$$

The determination of the exact correlation between B and the elastic properties of the components, as well as between p and l , the layer thickness, needs further work and consideration.

The success of the semi-empirical model (Equation 21) in the analysis of the experimental data indicates that the minimum cross-section concept is effective in most cases. This approach completely neglects stress concentrations and assumes homogeneous stress distribution in the composite. The averaging technique used in the theoretical model does basically the same and predicts properties equally well. These results indicate that interacting stress fields of neighbouring particles decrease the intensity of local stress concentrations leading to a more or less uniform stress distribution in the matrix. This, of course, can be higher than the external load or the one calculated from the minimum cross-section concept. It must be also noted

that small scale local yielding due to stress concentration might have the same result, i.e. averaging of local stresses acting in the matrix.

3.3. Debonding

As mentioned earlier, shear yielding can be accompanied or replaced by debonding in particulate filled composites [3–5]. Determination of the dominating micromechanical deformation mechanism is important in order to find optimum properties. It was shown that the critical stress for debonding, σ^D , is determined by thermal stresses, σ^T , and interfacial adhesion [6]

$$\sigma^D = -\frac{\sigma^T}{2} + \left(\frac{2G_0 W_{AB}}{C_1 R} \right)^{1/2} \quad (25)$$

where W_{AB} is the reversible work of adhesion and C_1 is a constant containing only geometrical parameters related to the extent of debonding. Substitution of the theoretical model into Equation 25 is very difficult since thermal stresses are also modified by the interphase having continuously changing properties. For a qualitative analysis, therefore, σ^T was neglected. Substituting Equation 18 into the debonding model one obtains

$$\sigma^D = \frac{1 - \phi}{1 - k\phi} \left(\frac{2G_0 W_{AB}}{C_1 R} \right)^{1/2} \quad (26)$$

Equation 26 leads to several conclusions. It indicates that composition dependence of shear yielding and debonding stress are the same, i.e. yield stress of the composite shows always the same compositional dependence irrespective of the mechanism of deformation. This implies also that separation of the two mechanisms is not possible using this evaluation technique.

Introducing the expression

$$k_1(R) = \left(\frac{2G_0 W_{AB}}{C_1 R} \right)^{1/2} \quad (27)$$

and transforming Equation 26 to the linear form one obtains

$$\frac{1 - \phi_f}{\sigma^D} = k_1(R) - k_1(R)k\phi_f \quad (28)$$

In this form the equation explains the particle size, A_f , dependence of the slope, k of the straight lines of Fig. 7, indicating also that the dominating deformation mechanism is debonding in the studied cases. Equation 28 shows, however, also that besides the slope, interception depends on particle size in the same way, a prediction not verified by the experimental results (Fig. 7). This contradiction sheds considerable doubt on the validity of the analysis of debonding in this form and indicates the necessity of further theoretical work.

Besides application of the model to debonding, further work has to be done in order to explain the particle size dependence of k . Effect of thermal stresses must be calculated and interacting stress fields of adjacent particles should be considered. A major

problem is the detection of a change in the micro-mechanical deformation mechanism, which definitely occurs as a function of particle size [4, 7], component properties or experimental conditions.

4. Conclusions

A model based on an interlayer with continuously changing properties was developed to describe stress-strain behaviour of heterogeneous polymer systems. Changing interlayer properties significantly alter deformation and stress fields around the particles.

By using a simple averaging procedure a correlation was derived which describes the compositional dependence of the yield stress of particulate filled composites. The equation contains two parameters related to the changing properties of the interphase and expresses relative load bearing capacity (stress transfer) of the matrix and the filler. The model properly predicts compositional dependence of yield stress; agreement with experimental data is good. Comparison of the theoretical model with an existing semi-empirical one indicates the development of a hard interlayer of constant thickness, which might explain the strong dependence of the parameter of the equation, k , on the specific surface area of the filler. Comparison of the two models justifies the averaging procedure used in the derivation of the compositional dependence of yield stress, as well. Application of the model to describe debonding was not successful. Further work has to be done to accommodate the effect of thermal stresses and interacting stress fields into the model, to apply it to debonding and to separate the effect of different micromechanical deformation processes on the measured yield stress of composites.

Acknowledgements

The National Scientific Research Fund of Hungary (Grant No. 1789) is greatly acknowledged for financial support of this project.

References

1. C. B. BUCKNALL, "Toughened plastics" (Applied Science, London, 1977).
2. A. J. KINLOCH and R. J. YOUNG, "Fracture behaviour of polymers" (Elsevier, London, 1983).
3. V. P. CHACKO, R. J. FARRIS and F. E. KARASZ, *J. Appl. Polym. Sci.* **28** (1983) 2701.
4. P. H. T. VOLLENBERG, PhD Thesis, Eindhoven University of Technology, Eindhoven, 1987.
5. B. PUKÁNSZKY, M. VAN ES, F. H. J. MAURER and G. VÖRÖS, *J. Mater. Sci.* **29** (1994) 2350.
6. B. PUKÁNSZKY and G. VÖRÖS, *Compos. Interfaces* **1** (1993) 411.
7. P. VOLLENBERG, D. HEIKENS and H. C. B. LADAN, *Polym. Compos.* **9** (1988) 383.
8. B. PUKÁNSZKY, *Makromol. Chem., Macromol. Symp.* **70/71** (1993) 213.
9. J. N. GOODIER, *J. Appl. Mech.* **55** (1933) 39.
10. B. PUKÁNSZKY, B. TURCSÁNYI and F. TÜDÖS, in "Interfaces in polymer, ceramic and metal matrix composites", edited by H. Ishida (Elsevier, New York, 1988) p. 467.
11. B. PUKÁNSZKY, *New Polym. Mater.* **3** (1992) 205.
12. B. PUKÁNSZKY, E. FEKETE and F. TÜDÖS, *Makromol. Chem., Macromol. Symp.* **28** (1989) 165.
13. B. PUKÁNSZKY, *Composites* **21** (1990) 255.
14. E. MORALES and J. R. WHITE, *J. Mater. Sci.* **23** (1988) 3612.
15. P. H. T. VOLLENBERG and D. HEIKENS, *Polymer* **30** (1989) 1656.
16. F. H. J. MAURER, in "Polymer composites", edited by B. Sedláček (Walter de Gruyter, Berlin, 1986) p. 399.
17. Y. TONG and I. JASIUK, in "Interphases in polymer, ceramic and metal matrix composites", edited by H. Ishida (Elsevier, New York, 1988), p. 757.
18. P. S. THEOCARIS, *Mater. Res. Soc. Symp. Proc.* **21** (1984) 847.
19. R. M. CHRISTENSEN, *J. Mech. Phys. Solids* **27** (1979) 315.
20. V. A. MATONIS, *Polym. Eng. Sci.* **9** (1969) 90.
21. F. H. J. MAURER, H. M. SCHOFFELEERS, R. KOSFELD and T. UHLENBROICH, in "Progress in science and engineering of composites", edited by T. Hayashi, K. Kawata and S. Umekawa (ICCM-IV, Tokyo, 1982) p. 803.
22. G. AKAY, *Polym. Eng. Sci.* **30** (1990) 1361.
23. K. IISAKA and K. SHIBAYAMA, *J. Appl. Polym. Sci.* **22** (1978) 3135.
24. K. F. MANSFIELD and D. N. THEODOROU, *Macromol.* **24** (1991) 4295.
25. O. ISHAI and L. J. COHEN, *J. Compos. Mater.* **2** (1968) 302.
26. L. NICOLAIS and M. NARKIS, *Polym. Eng. Sci.* **11** (1971) 194.
27. J. JANČAŘ, A. DIANSELMO and A. T. DIBENEDETTO, *ibid.* **32** (1992) 1394.
28. B. PUKÁNSZKY and F. TÜDÖS, *Makromol. Chem., Macromol. Symp.* **38** (1990) 221.
29. E. FEKETE, B. PUKÁNSZKY and Z. PEREDY, *Angew. Makromol. Chem.* **199** (1992) 87.

Received 31 January 1994
and accepted 15 March 1995